340 and 341 in "Free Radical Chemistry", Nonhebel, D. C., Walton, J. C., Eds., Cambridge University Press: Cambridge, 1974.
(17) Emmons, W. D. *J. Am. Chem. Soc.* **1957**, *79*, 5739.
(18) We cannot exclude at this time the possibility that brucine *N*-oxide might be a minor product formed in the reaction with the oxaziridine. The product isolated as described in ref 17, however, is shown to contain two atoms of chlorine by combustion analysis and displays ^{1}H NMR (270 MHz, D_2O) δ (HOD) 0.73 (2 H, AB q, J = 9.8 Hz, $^+NCH_2Cl$). Details of our study and a revised mechanism for the kinetic resolution of 2-*n*-propyl-3-methyl-3-isobutyloxaziridine by brucine will be published later.
(19) Böhme, H.; Boll, E. *Chem. Ber.* **1957**, *90*, 2013.
(20) The quantum yield (determined by ferrioxalate actinometry) for the photoreduction of **1** (436-nm narrow band-pass filter used) to flavin by tribenzylamine, $\phi \simeq 1.1$ (ϕ based on quantization of benzaldehyde formed from the *tert*-amine, at ~5% completion).
(21) See Bright, H. J.; Porter, D. J. T. *Enzymes, 3rd Ed.* **1975**, *8*, 421–505.

W. H. Rastetter,* T. R. Gadek, J. P. Tane, J. W. Frost
Department of Chemistry
Massachusetts Institute of Technology
Cambridge, Massachusetts 02139
Received September 14, 1978

Aspects of Artificial Photosynthesis. Photoionization and Electron Transfer in Dihexadecylphosphate Vesicles

Sir:

Initial steps of solar energy conversion have been modeled by photoionizing aromatic hydrocarbons in aqueous micelles.[1-7] Experiments have been prompted by the recognized abilities of micelles to solubilize apolar molecules and to affect rates of reactions.[8] Micelles had two important functions. Firstly, solubilization in their hydrophobic environment was expected to decrease the ionization potential. Secondly, subsequent to photoejection, electron-cation radical recombination was considered to be prevented by Coulombic repulsions at the charged micellar surface. Photoionization of pyrene[2,3] has been investigated in aqueous micellar sodium dodecyl sulfate in detail. There was a relatively high yield of ionization and the anionic surface of the micelle decreased charge recombinations. Photoionization was, however, biphotonic and did not, consequently, result in a lowering of the ionization potential. One would also expect efficient photoionization in liposomes.[9] Experimental results did not, however, fulfill this expectation. Photoionization yields in liposomes were relatively low and the process for pyrene was biphotonic.[10-12]

This communication reports the efficient *monophotonic ionization* of pyrene, localized in the hydrophobic bilayers of completely synthetic dihexadecylphosphate, DHP, vesicles.[13] In this environment the ionization potential of pyrene is substantially lowered. Equally significantly, photoejected electrons are shown to exit the vesicle interior and to be transferred to an acceptor. DHP vesicles may well represent one of the simplest functional models[14] for mimicking photosynthesis.[15]

Figure 1 shows transient absorption spectra of argon-saturated DHP-solubilized pyrene[16] following excitation by a 8-ns nitrogen laser at 337.1 nm.[17] In the 400-500 nm region of the spectra, there are three bands whose maxima are centered at 410, 450, and 480 nm. These absorptions are attributable[1] to the triplet-triplet transition of pyrene (410 and 480 nm) and to pyrene cation radical (450 nm). Assignments were confirmed by the addition of base (pH 10). Only the decay rate of the 450 absorbing species increased.[18] The broad absorption band in the red is due to the hydrated electron, e^-_{aq}.[19] This absorption is removed by the addition of oxygen. The insert in Figure 1 shows the linear dependence of the e^-_{aq} on the laser beam intensity.[20] Evidently, absorption of only one 337.1-nm photon of 3.68-eV energy is required to ionize DHP-entrapped pyrene in the intensity range investigated. The ionization threshold of a solute, I_s, is given by[22]

$$I_s = I_g + P_+ + V_0 \quad (1)$$

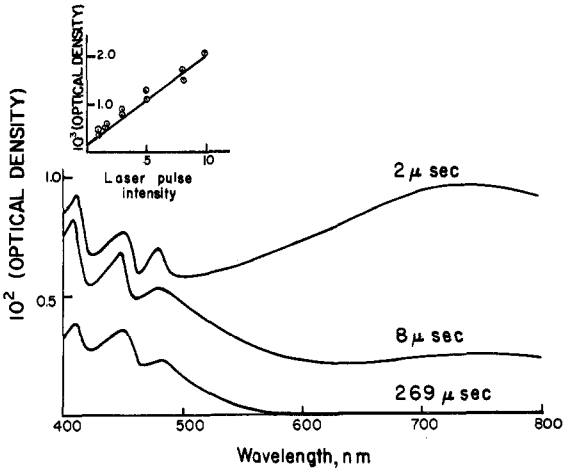

Figure 1. Absorption spectra of the transient formed on excitation of pyrene, localized in DHP vesicles. The peak laser output was 2.3 mJ per pulse. The insert shows the electron yield at 670 nm as a function of laser pulse intensity.

where I_g is the gas phase ionization potential of the solute (I_g (pyrene) = 7.55 eV),[2] P_+ is the polarization energy of the solute cation (P_+ (pyrene) = −1.6 eV),[2] and V_0 is the energy state of the electron in solution (V_0 (decane) = 0.22 eV).[23] Substituting these values to eq 1 results in I_s = 6.17 eV. Thus, the energy lowering of the ionization potential is 2.49 eV. The lowering of the ionization potential is a composite effect of alteration of the values of V_0 and P_+. Since the hydrated electron is in fact monitored in water, the value of V_0 in the vesicle can approach that in water (−1.5 eV).[24] Pyrene molecules are dynamically distributed in the vesicles; at a given time some of them may well be in close proximity to the charged polar head groups. A similar effect has been observed by Thomas and Piciulo.[7] Additional energy may be gained from the electrostatic stabilization of the pyrene cation radical by the negatively charged phosphate head group on the vesicles.

The photoexcited electron decays by two consecutive first-order processes at or near the ambient temperature (Figure 2). Half-life times for these decays are 0.72 and 2.48 μs at 21 °C and 0.95 and 2.19 μs at 26 °C. Increasing the temperature increased the contribution of the slow electron decay until the process became monoexponential (Figure 2). These results can be rationalized in terms of altered reaction sites of the electron as a function of temperature-induced morphological changes of the DHP vesicle. Above the phase temperature (46 °C, for example) the bilayers of the vesicle become fluid. All the electrons can, therefore, readily exit and decay in the bulk aqueous phase monoexponentially, by reacting with impurities (unremoved oxygen and titanium from sonication) and with each other. This monoexponential decay corresponds to the long-lived component (Figure 2). At lower temperatures, the surfactant vesicle is more rigid and their head groups are closer together. Under these circumstances, some of the electrons are scavenged by protons, concentrated at the surface of the negatively charged DHP vesicles. Using the observed half-life time for the fast electron decay ($t_{1/2} = 0.95 \times 10^{-6}$ s at 26 °C) and the rate constant ($k_{e^-_{aq}+H^+} = 2.0 \times 10^{10}$ M^{-1} s^{-1})[25] leads to an apparent proton concentration of 3.6×10^{-5} M. Such a degree of proton concentration has been demonstrated for aqueous anionic micellar sodium dodecyl sulfate[26] and is entirely expected for the much larger[27] DHP vesicles.

In separate experiments transfer of the photoejected electron to benzophenone has been demonstrated. External addition of benzophenone[28] to pyrene-containing DHP vesicles resulted in the exponential decrease of the half-life time of the hydrated electron (to a value of 0.4 μs) with the concurrent appearance

0002-7863/79/1501-2231$01.00/0

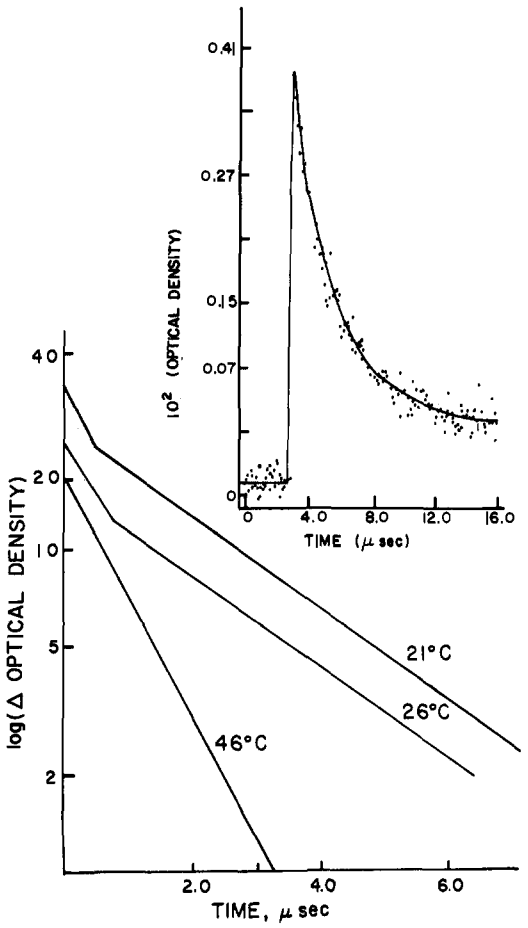

Figure 2. Decay of photoejected hydrated electron at different temperatures. The insert shows a typical digitalized electron decay at 26 °C.

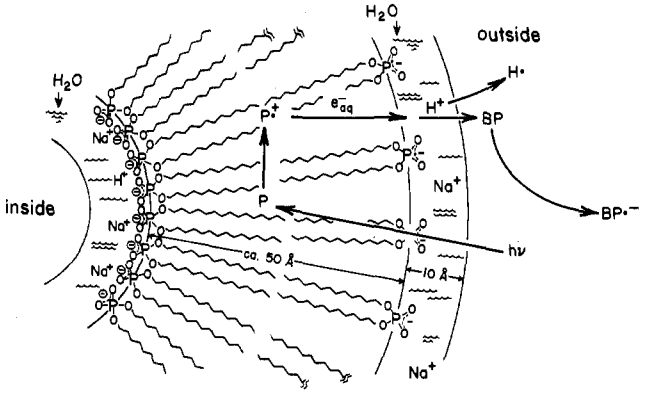

Figure 3. Schematic representation of laser-induced photoionization of DHP entrapped pyrene and subsequent electron transfer. Pyrene molecules are shown to be localized in the center of the bilayer. In reality, this probe is free to distribute itself dynamically and some probe may be localized somewhat close to the head group of the vesicle.

of a long-lived ($t_{1/2} \geq 220$ μs) species having an absorption maximum at 610 nm. The new transient corresponds to the benzophenone anion radical.[29]

Figure 3 shows the schematics of the proposed pyrene photoionization and subsequent electron transfers. Beneficial effects of this exceedingly simple surfactant vesicles are manifold. The predominant localization of pyrene in the hydrophobic interior results in monophotonic electron ejection and a substantial lowering of the ionization potential.[30] The polarity gradient provides driving force for the exit of the electron and the net negative charge on the DHP vesicles prevents charge recombination. There are at least two alternatives for subsequent conversions of the electron. Reactions with protons give rise to hydrogen atoms and ultimately to molecular hydrogen. Feasibility of electron transfer has been demonstrated using benzophenone. Other acceptors may provide a self-regenerating cycle. In addition, components of oxidation and reduction cycles can be separated on either side of the DHP vesicle. These and other aspects of artificial photosynthesis are being actively pursued in our laboratories.

Acknowledgments. Support of the National Science Foundation and the Robert A. Welch Foundation is gratefully acknowledged. Experiments were carried out at the Center for Fast Kinetics Research at The University of Texas at Austin. This center is supported by National Institutes of Health Grant RR00886 from the Biotechnology Resources Program of the Division of Research Resources and by the University of Texas at Austin. We have greatly benefited from helpful discussions with Professor P. P. Infelta.

References and Notes

(1) For recent reviews see (a) M. Grätzel and J. K. Thomas in "Modern Fluorescence Spectroscopy.", Vol. 2, E. L. Wehry, Ed., Plenum Press, New York, 1976, p 196; (b) M. Grätzel in "Micellization, Solubilization, and Microemulsions", K. L. Mittal, Ed., Plenum Press, New York, 1977, p 531; (c) K. Kalyanasundaran and J. K. Thomas in ref 1b, p 569.
(2) S. C. Wallace, M. Grätzel, and J. K. Thomas, *Chem. Phys. Lett.*, **23**, 359 (1973).
(3) M. Grätzel and J. K. Thomas, *J. Phys. Chem.*, **78**, 2248 (1974).
(4) S. A. Alkaitis, G. Beck, and M. Grätzel, *J. Am. Chem. Soc.*, **97**, 5723 (1975).
(5) S. A. Alkaitis, M. Grätzel, and A. Henglein, *Ber. Bunsenges. Phys. Chem.*, **79**, 541 (1975).
(6) S. A. Alkaitis and M. Grätzel, *J. Am. Chem. Soc.*, **98**, 3549 (1976).
(7) J. K. Thomas and P. Piciulo, *J. Am. Chem. Soc.*, **100**, 3239 (1978).
(8) J. H. Fendler and E. J. Fendler, "Catalysis in Micellar and Macromolecular Systems", Academic Press, New York, 1975.
(9) A. D. Bangham, *Prog. Biophys. Mol. Biol.*, **18**, 29 (1968); A. D. Bangham, M. W. Hill, and N. G. A. Hill in "Methods in Membrane Biology", Vol. 11, E. D. Korn, Ed., Plenum Press, New York, 1974, p 38.
(10) S. Cheng and J. K. Thomas, *Radiat. Res.*, **60**, 268 (1974).
(11) S. Cheng, J. K. Thomas, and C. F. Kulpa, *Biochemistry*, **13**, 1135 (1974).
(12) D. J. W. Barber, D. A. N. Morris, and J. K. Thomas, *Chem. Phys. Lett.*, **37**, 481 (1976).
(13) R. A. Mortara, F. H. Quina, and H. Chaimovich, *Biochem. Biophys. Res. Commun.*, **81**, 1080 (1978).
(14) For the description and characterization of completely synthetic surfactant vesicles, see K. Tamaki, F. Kumamuru, and T. Takayanagi, *Chem. Lett.*, 387 (1977); T. Kunitake and Y. Okahata, *J. Am. Chem. Soc.*, **99**, 3860 (1977); K. Deguchi and J. Mino, *J. Colloid Interface Sci.*, **65**, 155 (1978); C. D. Tran, P. L. Klahn, A. Romero, and J. H. Fendler, *J. Am. Chem. Soc.*, **100**, 1622 (1978); A. Romero, C. D. Tran, P. L. Klahn, and J. H. Fendler, *Life Sci.*, **22**, 1447 (1978); Y. Y. Lim and J. H. Fendler, *J. Am. Chem. Soc.*, in press; K. Kano, A. Romero, B. Djermouni, H. Ache, and J. H. Fendler, *J. Am. Chem. Soc.*, in press.
(15) For a recent utilization of liposomes to model photosynthesis, see G. Porter and M. V. Archer, *Interdiscip. Sci. Rev.*, 1, 119 (1976); M. Calvin, *Acc. Chem. Res.*, **10**, 369 (1978); W. E. Ford, J. W. Otvos, and M. Calvin, *Nature (London)*, **274**, 507 (1978).
(16) Pyrene-containing DHP vesicles were typically prepared by dissolving 5.0 mg of DHP and 0.02 mg of pyrene in 1.0 mL of chloroform. Subsequent to solvent evaporation, the thin lipid film was removed by shaking with 2.0 mL of triply distilled water. The turbid suspension was sonicated for 30 min at temperatures >60 °C by means of the microprobe of a Braunsonic 1510 sonifier set at 70 W. The undispersed DHP was removed by centrifugation at 5000 rpm in an International clinical centrifuge for 10 min. The concentration of the pyrene was adjusted to $\sim 10^{-4}$ M by dilution with H_2O. The pH was adjusted to 7.0 by NaOH.
(17) A. A. Gorman and M. A. J. Rodgers, *Chem. Phys. Lett.*, **55**, 52 (1978).
(18) The lifetime of pyrene cation radical was in the order of milliseconds.
(19) E. J. Hart and M. Anbar, "The Hydrated Electron", Wiley, New York, 1970.
(20) The slight intercept on the *y* axis is the result of residual triplet absorption. Biphotonic ionization would result in an intercept in the *y* axis.[21] At the energy absorbed, the photoconversion is <1%. No appreciable depletion of pyrene occurred therefore.
(21) U. Lachish, A. Shafferman, and G. Stein, *J. Chem. Phys.*, **64**, 4205 (1976).
(22) B. Raz and J. Jortner, *Chem. Phys. Lett.*, **4**, 155 (1969).
(23) R. A. Holroyd and W. Taucherti, *J. Chem. Phys.*, **60**, 3715 (1974); since pyrene is embedded in the hydrophobic parts of the DHP vesicle, its environment is likely to be hydrocarbon-like; thus using a value for decane is not unreasonable.
(24) G. C. Barker, G. Bottura, G. Cloke, A. W. Gardner, and M. J. Williams, *Electroanal. Chem. Interfac. Electrochem.*, **50**, 232 (1974).
(25) M. Anbar, M. Bambenek, and A. B. Ross, "Selected Specific Rates of Reactions of Transients from Water in Aqueous Solution", *Natl. Stand. Ref. Data Ser., Natl. Bur. Stand.*, **43** (1973).
(26) C. A. Bunton, K. Ohmenzetter, and L. Sepulveda, *J. Phys. Chem.*, **81**, 2000 (1977).

(27) Taking the radius of a DHP vesicle to be 250 Å and the bilayer thickness to be 50 Å, we calculate that each vesicle contains 18 000 surfactant molecules and has external and internal areas of 7.85×10^5 and 5.02×10^5 Å^2, respectively. At the preparations used ([DHP] = 2.28×10^{-3} M), the vesicle concentration is 1.24×10^{-7} M. Thus, each vesicle contains ~800 pyrene molecules.
(28) The stoichiometric concentration of benzophenone varied between 3 and 10×10^{-6} M^{-1}. Benzophenone distributes itself, of course, between the bulk solvent and the surface of the vesicle. The average decrease between pyrene and benzophenone is rather small since, on the time scale of our observation (2 ns), we could not see the buildup of the transient absorption at 610 nm (owing to the benzophenone anionic radical).
(29) G. E. Adams, J. H. Baxendale, and J. W. Boag, *Proc. R. Soc. London, Ser. A*, **277**, 549 (1964).
(30) At laser intensities of 50–150 mJ per pulse (~50- to 70-fold higher intensities than those used in the present work), photoionization of pyrene in anionic micellar sodium dodecyl sulfate was shown to be biphotonic.[31] The observed monophotonic ionization of 3-aminoperylene[7] was suggested to be the consequence of an apparent change in the order of photoionization from biphotonic to monophotonic as a result of decrease of charge recombination caused by the micelle.[31]
(31) G. E. Hall, *J. Am. Chem. Soc.*, **100**, 8262 (1978).

Jose R. Escabi-Perez, Alejandro Romero
Sava Lukac, Janos H. Fendler*
Department of Chemistry, Texas A&M University
College Station, Texas 77843
Received November 7, 1978

Is Formamide Planar or Nonplanar?

Sir:

The structure of formamide (NH_2CHO, **1**) is of fundamental importance in organic chemistry, particularly as a prototype for polypeptides; surprisingly, it has remained unresolved over many years. Indeed, three microwave spectral investigations over the past 20 years have led to alternating views on the planarity or nonplanarity of this molecule.[1-4] In the first of these studies in 1957, a planar structure was assumed,[1] but a subsequent study[2] in 1960 favored a nonplanar structure. This latter was (and continues to be) widely accepted.[5] It was not seriously challenged until 1974 when a redetermination[3] of the microwave spectrum returned to an interpretation in terms of a planar structure. In this communication, we use ab initio molecular orbital calculations to show that formamide lies in a very flat potential well in the vicinity of a planar structure.

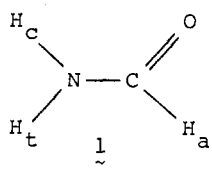

1

There have been numerous previous ab initio studies of formamide. Most of these have used a fixed (experimental or model) geometry[5-7] or have carried out optimizations on a structure assumed to be planar.[8] As far as we are aware, the only calculation[9] which included extensive geometry optimization and allowed for nonplanarity utilized a minimal basis set which, as we shall see, is not really adequate for situations of this type. On the other hand, it is encouraging to note that the structure and inversion barrier in ammonia itself have been shown to be well described within the Hartree-Fock approximation.[10,11] As NH_2CHO is a formyl-substituted ammonia molecule, it seems reasonable to expect that the inversion process in formamide might be similarly well described. Our strategy here has been to carry out self-consistent-field calculations[12-14] on formamide with full-geometry optimization at increasing levels of sophistication in the basis set. We use, as a measure of the significance of the individual formamide calculations, the performance of the same basis set for ammonia where the experimental situation is more clearly defined.[15,16] Optimized structural and energy data are presented in Tables I (NH_3) and II (NH_2CHO).

We note the following points. (1) Our initial optimizations with the minimal STO-3G basis set[17] yielded a nonplanar structure (Table II) for formamide. The STO-3G basis is, however, known to underestimate valence angles at heteroatoms and, in particular, for ammonia[18] this leads (Table I) to an underestimation of the HNH angles and an inversion barrier that is too high. For this reason, STO-3G would be expected to exaggerate the degree of nonplanarity in a molecule

Table I. Optimized Structural and Energy Data for Pyramidal (C_{3v}) and Planar (D_{3h}) Forms of Ammonia[a]

	STO-3G[b]	4-31G[c]	4-31G/BF	DZ + d	DZP	HF[d]	exptl[e]
r(N—H) (C_{3v})	1.033	0.991	1.002	1.003	1.000	0.999	1.012
∠HNH (C_{3v})	104.2	115.8	109.8	107.3	108.1	107.7	106.7
r(N—H) (D_{3h})	1.006	0.986	0.988	0.991	0.987	0.984	
E (C_{3v})	−55.45542	−56.10669	−56.12892	−56.19972	−56.20991	−56.22333	
E (D_{3h})	−55.43767	−56.10600	−56.12398	−56.18958	−56.20200	−56.21504	
barrier	11.1	0.4	3.1	6.4	5.0	5.2	5.8

[a] Bond lengths are given in Ångstroms, bond angles in degrees, total energies in hartrees, relative energies (barriers) in kcal mol^{-1}. [b] From ref 18. [c] From ref 19. [d] Near Hartree-Fock results from ref 10c. [e] From ref 15 and 16.

Table II. Optimized Structural and Energy Data for Formamide[a]

	STO-3G	4-31G	4-31G/BF	DZ + d[b]	DZ + d[c,d]	exptl[e]
r(N—C)	1.436	1.346	1.346	1.355	1.358	1.352 ± 0.012
r(C=O)	1.216	1.216	1.191	1.197	(1.197)	1.219 ± 0.012
r(N—H$_c$)	1.027	0.993	0.995	0.996	(0.996)	1.002 ± 0.003
r(N—H$_t$)	1.026	0.990	0.991	0.994	(0.994)	1.002 ± 0.003
r(C—H$_a$)	1.104	1.081	1:091	1.089	(1.089)	1.098 ± 0.010
∠H$_c$NC	111.6	119.5	119.4	119.3	118.3	118.5 ± 0.5
∠H$_t$NC	112.1	121.9	121.7	121.5	120.4	120.0 ± 0.5
∠NCO	123.9	124.7	125.0	124.8	(124.8)	124.7 ± 0.3
∠NCH$_a$	111.9	113.7	113.7	112.8	112.8	112.7 ± 2.0
∠H$_c$NCO	21.5	0	0	0	9.1	0
∠H$_t$NCO	145.1	180	180	180	168.8	180
∠H$_a$CNO	176.6	180	180	180	178.7	180
energy	−166.69184	−168.68159	−168.75398	−168.96554	−168.96558	

[a] Bond lengths in Ångstroms, bond angles in degrees, total energies in hartrees. [b] Planar structure. [c] Nonplanar structure. [d] Values in parentheses not reoptimized for nonplanar structure. [e] From ref 3.

0002-7863/79/1501-2232$01.00/0